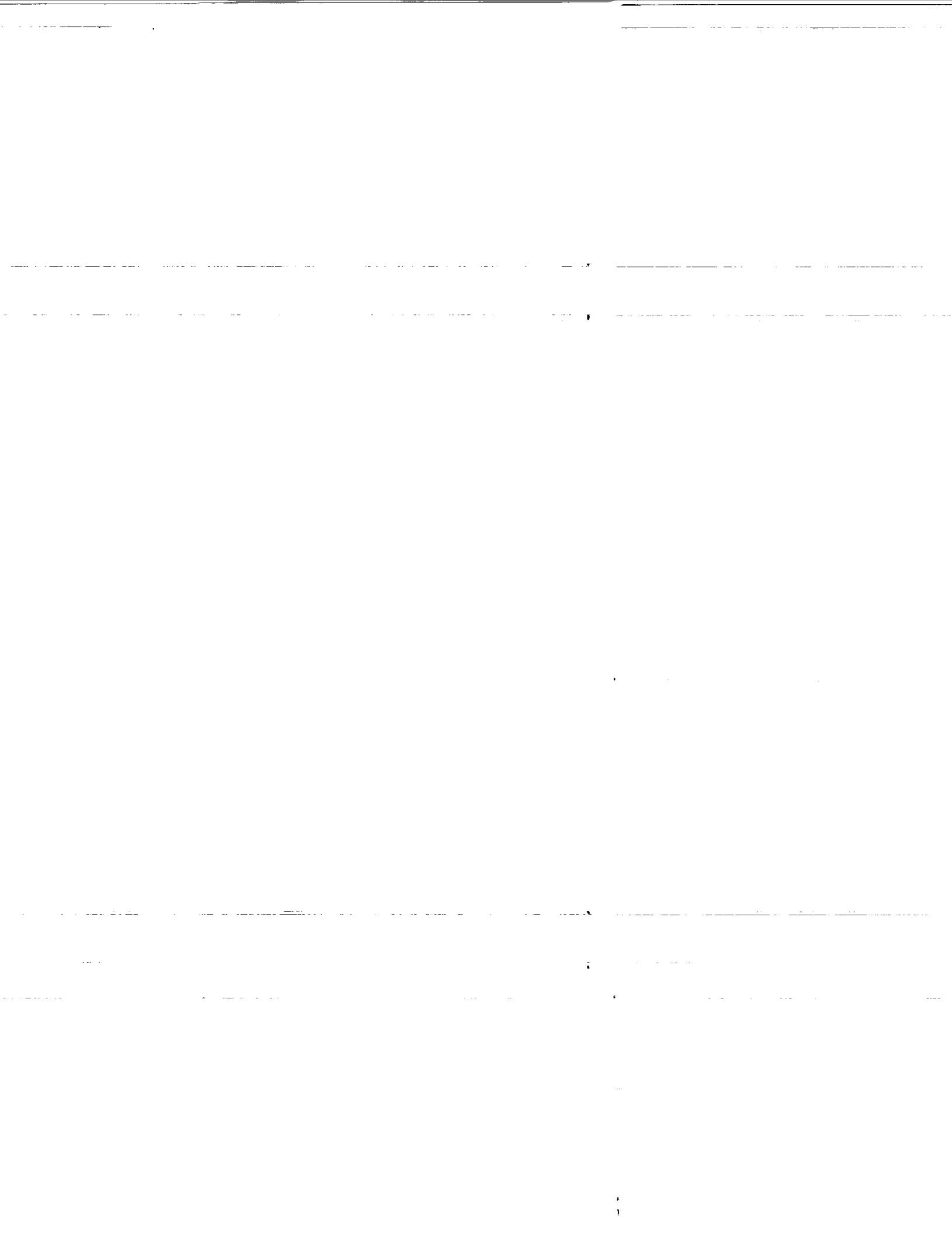/N-38

/4945

P·13

A Preliminary Investigation of Acousto-Ultrasonic NDE of Metal Matrix Composite Test Specimens

Harold E. Kautz and Brad A. Lerch
Lewis Research Center
Cleveland, Ohio

May 1991

NASA

A PRELIMINARY INVESTIGATION OF ACOUSTO-ULTRASONIC NDE OF METAL

MATRIX COMPOSITE TEST SPECIMENS

Harold E. Kautz and Brad A. Lerch
Lewis Research Center
Cleveland, Ohio 44135

SUMMARY

Acousto-ultrasonic (AU) measurements were performed on a series of [0]$_8$, [90]$_8$, [±30]$_{2s}$, [±45]$_{2s}$, [±60]$_{2s}$, [0/90]$_{2s}$, and [90/0]$_{2s}$ tensile specimens composed of eight laminated layers of continuous, SiC fiber reinforced Ti-15-3 matrix. The frequency spectrum was dominated by frequencies of longitudinal wave resonance through the thickness of the specimen at the sending transducer, while signal propagation from the sender to the receiver was by shear waves. The magnitude of the frequency spectrum of the AU signal was used for calculating a stress-wave factor (SWF) based upon integrating the spectral distribution function. The SWF was sensitive to fiber/matrix debonding due to mechanical strain and also to unconstrained thermal cycling. Damage in this MMC structure due to tensile loading or thermal cycling was detected by this change in the magnitude of the frequency spectrum. A measure of the speed of the acousto-ultrasonic pulse between the sending transducer and the receiver was obtained by calculating mean time, or first moment, in the time domain signal. This parameter shows some sensitivity to the stiffness of the tensile specimens. This sensitivity to stiffness needs further study.

INTRODUCTION

An approach to improving reliability and reproducibility of structures is to utilize nondestructive evaluation (NDE) techniques during research and development. An NDE technique can sometimes be substituted for a destructive test (see, e.g., ref. 1). This procedure not only can affect a savings in research time and material resources, but can also lead to a more fundamental understanding of the parameters that determine strength and life.

Acousto-Ultrasonics (AU) is a technique that was devised to meet the particular problems associated with NDE of composites such as the need to evaluate the strength and integrity of internal interfaces (ref. 2). It has proven sensitive to strength parameters such as interlaminar shear strength (refs. 3 and 4), and damage conditions such as transply crack density (ref. 5). All such results have been previously obtained on fiber reinforced polymeric resin structures. It is the object of the present investigation to determine to what extent the technique can be applied to metal matrix composites (MMCs), and in particular, to typical tensile specimen geometries employed in research and development of this material.

EXPERIMENTAL

Acousto-Ultrasonic Technique

The AU technique, as it is practiced at NASA Lewis, has been described in detail elsewhere (ref. 3). AU uses two piezoelectric transducers, as shown in figure 1. The sender introduces ultrasonic pulses into the tensile specimen. The pulses move in the length direction of the specimen and are sampled by the receiver, as shown in figure 2. This collected and digitized waveform is the AU signal.

In the present work, the ultrasonic pulse and waveform digitizer sweep were initiated from a Panametrics 5052PRX pulser. It was set at minimum repetition rate of 500 Hz, damping = 6, and energy level set at 4. The receiving transducer output was amplified using two 25 dB amplification stages of an HP model 8447D having a bandwidth of 0.1 to 1300 MHz and then sent to a Tektronics 7912AD digitizer.

The transducers were coupled to the tensile specimen surface through elastomeric pads with a force of 12 N. This force on the pads is in a range that produces minimal fluctuation in coupling efficiency. The pads were 1.27 cm long by 0.3 cm wide strips, and were 0.1 cm thick when not under the force. For all fiber orientations, the ultrasonic path from sender to receiver was parallel to the loading axis of the specimen. Three transducer combinations were employed. They were: 5 MHz sender with 2.25 MHz receiver, 2.25 MHz sender with 2.25 MHz receiver, and 2.25 MHz sender with 1 MHz receiver. For all three combinations the transducer centerline separation was maintained at 1.91 cm. The most useful data were acquired with a 5-MHz broad band sending transducer and a 2.25 MHz broad band receiving transducer.

For each set of conditions described above, and on each specimen measured at each processing step, six AU waveforms were collected. Three were collected on each side. Because of alternating sides between measurements, the transducers were recoupled to the specimen before each measurement. Data presented here are averages of six values. Error bars represent one standard deviation of the values.

Materials Tested

The metal matrix composite was a SiC(SCS-6) reinforced Ti-15V-3Cr-3Sn-3Al (Ti-15-3) material which contained eight rows of fibers, yielding a total composite thickness of 0.20 cm. The nominal fiber volume fraction was 34 percent.

Additional microstructural details of this material can be found in references 6 and 7. Room temperature tensile tests were performed on $[0]_8$ and $[\pm30]_{2s}$ as well as a fewer number of tests on $[\pm45]_{2s}$, $[\pm60]_{2s}$, $[0/90]_{2s}$, and $[90]_8$ layups. Two specimen designs were employed; the first being a 1.27-cm wide, straight-sided specimen, and the second a specimen having a reduced gauge section. The gauge width in the reduced section was 0.76 cm. Selected specimens were given a heat treatment of 700 °C for a 24-hr period in vacuum, the remainder of the specimens were tested in the as-fabricated condition. Testing was performed in a servohydraulic machine under a constant total strain rate of $1\times10^{-4}/$ sec. Strain was measured using an extensometer which was mounted on the edge of the specimen. Some tests were interrupted prior to failure and examined using AU to determine if the development of damage could be detected.

Two $[90/0]_{2s}$ (the first number is the fiber orientation in the outermost ply) specimens were thermally cycled by repeatedly lowering and raising them into and out of a furnace. These specimens were cycled between 200 and 1000 °F for 2000 cycles.

RESULTS AND DISCUSSION

Acousto-Ultrasonic Signal Analysis

Figure 2 shows a typical time domain waveform and figure 3 is its magnitude spectrum. The spectra for this combination of AU parameters always exhibited two peaks. In the case of the unidirectional tensile specimens, for example, one peak was at 1.6 MHz and the other was at 3.1 MHz. The broadband transducer combination: 5 MHz sender/ 2.25 MHz receiver was the most favorable for resolving these frequency peaks. It appears that the 1.6 MHz peak is the fundamental frequency for standing wave resonance through the specimen thickness at the sending transducer and that the 3.1 MHz peak is the first harmonic. One might expect a series of higher order

peaks to appear in the spectrum. As it turns out, a small second harmonic sometimes does appear. In general, however, the spectrum is subject to the response range of the transducers and to the attenuation in the specimen as well as in the elastic couplant pads. These factors preclude the presence of a series of higher order harmonic peaks.

It is believed that the ultrasonic energy travels from the standing wave region under the sender to the receiver by means of shear waves with their displacement vector oriented the same as that of the standing waves. This is illustrated in figure 4. There are two indications that this model is correct. First, rough measurement of the velocity of the pulses in the specimen length direction indicates that it is between 0.2 and 0.4 cm/µsec. This range includes the expected shear wave velocity for Ti of 0.312 cm/µsec (ref. 8). The second indication comes from an additional experiment performed on a thick panel. With the sending transducer coupled in the usual AU configuration, a shear wave transducer was coupled to the edge as a receiver. Its response was strong when it was oriented for normal-to-surface wave displacements, but weak for in-plane displacements. The experiment showed that an important mode of ultrasound propagation from the sender to the receiver is by shear waves that have the same frequency distribution, and displacement vector direction, as the longitudinal waves resonating under the sender. They may be considered Lamb Waves. Lamb waves have earlier been shown useful in AU analysis (refs. 9 and 10).

From the above model of the spectrum one can calculate a through-thickness longitudinal wave ultrasonic velocity for the tensile specimens. If the fundamental peak is at f_1, the first harmonic peak is at f_2, and the specimen thickness is t, then the through thickness velocity can be calculated from either peak.

From the fundamental:

$$V = 2tf_1 \qquad (1)$$

From the first harmonic:

$$V = tf_2 \qquad (2)$$

The high frequency peak gave more reproducible velocities from specimen to specimen than did the low one. The value was approximately 0.66 cm/µsec for all ply orientations.

Preliminary investigations with SiC/ Ti-15-3 panels of significantly greater thickness agree with the assumptions used above. For example, a SiC/Ti-15-3 panel four times as thick produces an AU frequency spectrum with a fundamental peak at about one fourth of the frequency (i.e., at 0.4 MHz). Applying equations (1) or (2) to the thicker panel yields a velocity of about 0.66 cm/µsec, identical to that found in the thin tensile specimens. These results compare with a longitudinal velocity of 0.58 cm/µsec obtained for the same calculation on the AU spectrum obtained with a panel of Ti-15-3 matrix material and 0.57 cm/µsec for pure titanium. These results are in close agreement with the range of 0.57 to 0.61 cm/µsec found for various Ti alloys with conventional pulse-echo measurements (refs. 11 and 12).

These through-thickness velocity results are summarized in table I along with an estimate velocity calculated from the known properties of the composite's constituents. The calculation assumes that the wave passes through SiC for 34 percent of the thickness with a velocity of 1.2 cm/µsec and through the Ti-15-3 for the remaining 66 percent of the distance at 0.57 cm/µsec. The velocity through the composite is then calculated by the rule of mixtures. This calculation sets an upper bound for the through thickness velocity in the composite. The measured velocity in the composite was larger than that measured for

the matrix material, suggesting that the fibers affect the wave propagation. However, they do not play as large a role as one would expect from the rule of mixtures calculation. This may be an indication of fiber/matrix debonding or porosity within the material. The difference in calculated velocity may also be caused by other phases which have not been taken into account (e.g., the c-core in the fiber or phases at the fiber/matrix interface), but which may affect the velocity.

Tensile Behavior

Typical stress-strain plots for the $[0]_8$ and $[\pm30]_{2s}$ are shown in figure 5. The tensile behavior for the $[0]_8$ specimens is approximately linear to failure (failure is defined in this paper as separation of specimen into two pieces). A small nonlinearity does exist near the ultimate tensile stress. The $[\pm30]_{2s}$ specimens show a nonlinear behavior almost from the beginning of the test. Occasionally, a sudden load drop would appear in the tensile curve (see, e.g., the $[\pm30]_{2s}$ specimen in fig. 5) which was associated with an audible click. This occurred in both orientations and did not occur at any particular stress/strain level. A summary of the tensile properties for the specimens of all the layups investigated is given in table II. The elastic modulus, E, was calculated using a least squares analysis of the initial, linear portion of the stress-strain curve.

Acousto-Ultrasonics and Interrupted Tensile Tests

For the tensile specimens, stress-wave factors (SWF) were calculated by integrating the magnitude spectrum, G(f):

$$SWF = \int_a^b G(f)df \qquad (3)$$

This was done for various limits of integration, a and b as indicated later.

Several specimens were interrupted during tensile testing and examined using acousto-ultrasonics. All of these specimens were strained into the nonlinear elastic region, that is, the instantaneous tangent modulus at these strains is lower than the original elastic modulus. Table III lists them along with their strain at interruption and, where available, a summary of the observations from subsequent metallographic examination. Metallography showed (ref. 13), that the primary form of observable degradation present in each case was debonding. It should be noted that the degrees of debonding listed in table III are qualitative. A quantitative description is not possible since there is a resolution problem associated with the earlier stages of debonding. In addition, only certain portions of the interface along the fiber debond, which depend upon the local stress conditions and bond strengths.

Figure 6 shows the acousto-ultrasonic stress-wave factor in both the before tested state and after some degree of tensile straining. These SWF values were calculated employing equation (3) with $a = 0$ and $b = 12.8$ MHz (the total spectrum). The $[0]_8$ specimens show some decrease in the SWF after straining, but the change is statistically insignificant. In addition, the specimen which was strained to near failure (specimen E7) and which has some evidence of damage shows the same degree of change in the SWF, if not less, than the specimen which was strained just past the proportional limit (specimen 3) and showed no evidence of damage.

Both the $[90]_8$ specimens show significant changes in the SWF after straining. Specimen 40, which was strained to 1.00 percent, showed a larger decrease in the SWF than specimen 39 which was only strained to 0.60 percent. This change corresponds to the observed difference in damage states between these two specimens, the damage being much more extensive in specimen 40.

There were three $[\pm30]_{2s}$ specimens in the interrupted tests. Of them, only specimen 13, strained to 0.61 percent,

4

showed a statistically significant decrease in SWF from before the test. Specimen 10 was strained to 0.5 percent and showed slight amounts of debonding similar to specimen 13. However, the decrease in SWF was not statistically significant. The third [±30]$_{2s}$ specimen, D10, showed no change in SWF in going from before the test to the final state of 0.80 percent strain despite the fact that after the test extensive debonding was observed.

These experiments suggest that the amount of damage due to tensile straining can be identified using the AU technique. However, the issue of reducing the scatter in the SWF observed in some specimens must first be addressed before this technique can be used effectively. This scatter can result from various sources, some of which could be specimen to specimen variation in: (1) residual stresses, (2) warpage in the specimens, and (3) surface finish. These sources may also influence the degree of change between the initial state and the damaged state.

Acousto-Ultrasonics and Thermally Cycled Specimens

Two ([90/0]$_{2s}$) specimens were measured with acousto-ultrasonics before and after thermal cycling. The SWF for the integration limits of a = 2.56 and b = 5.12 MHz in equation (3) (i.e., including the first harmonic peak) was found to decrease due to the thermal cycling step. Figure 7 shows this result in terms of a normalized SWF where the SWF integral with limits of a = 2.56, b = 5.12 is divided by the SWF with limits of a = 0 and b = 12.8 MHz. Based on an earlier investigation (ref. 14), the thermal cycling is expected to produce some interfacial debonding as well as a few, isolated matrix cracks. However, this limited form of damage did not influence the residual tensile properties as was indeed shown by subsequent tensile tests (see, e.g., table II). Therefore, the AU method is capable of detecting small amounts of damage in this material

which would not be evident by performing coarser, destructive tests. The SWF in the range of the fundamental peak was relatively unchanged, again suggesting that higher frequencies may be more effective in detecting damage.

Acousto-Ultrasonics and Stiffness

Since the stiffness effects ultrasonic velocity, the aspect of the AU signal most likely to be modulus sensitive is the time of transit from sender to receiver and the first moment of the time domain signal, or mean arrival time. This signal is shown in figure 2.

This mean, $\bar{t}$, of the time domain signal wf(t) is:

$$\bar{t} = \frac{\int_0^T abs[wf(t)]t\, dt}{\int_0^T abs[wf(t)]dt} \qquad (4)$$

Where T is the time of the end of the signal record, in this case 20 μsec.

This equation (4) function is plotted versus tensile modulus for various ply layups in figure 8. Figure 8 shows that the higher the tensile modulus (and therefore also the higher the shear wave velocity along the length of the specimen), the earlier the AU signal arrives at the receiver. Note that specimens of five different layups are plotted in figure 8. The data indicate that the AU signal does not see specific fiber orientations but rather the resultant stiffness of the structure.

In figure 8, one data point lies to the right of the other data. This [0]$_8$ specimen (5) had an anomalously high modulus compared to the other unidirectional, [0]$_8$ specimens (i.e., 258 compared to an average modulus of 186 GPa). The fiber volume fraction of this specimen was the same as the other [0]$_8$ specimens (table II). Also, the matrix hardness for this specimen was identical

5

to all other specimens, excluding the possibility that either a change in the fiber or matrix properties or a different fiber volume fraction led to the high modulus. However, metallographic evaluation indicated that the reaction zone surrounding approximately half of the fibers in this specimen was larger than usual, having a thickness of ~3 μm (fig. 9) rather than the 0.3 μm observed in the other specimens (ref. 7). The reason for the large reaction zone is unknown. With all other factors being the same, this leads to the conclusion that the quality of the interface can significantly affect the elastic modulus of the composite. It also can be concluded that the AU method is capable of detecting such constituent anomalies, at least when they affect the stiffness of the composite.

Acousto-Ultrasonics and Specimen Geometry

The relationship between the thickness of the specimen and the shape of the AU frequency spectrum has already been discussed. Besides this it was found, as with other materials, that the signal strength, and hence also the absolute SWF, increases with the cross-sectional area of the path from sender to receiver. The use of the normalized SWF and mean time of arrival eliminates this geometry dependence since the dimensions cancel out between the numerator and the denominator in the calculation. In the present work this allowed the equivalent comparison of mean arrival times for specimens with both reduced gauge and straight sides which were considerably different in width.

CONCLUSIONS

Composite damage due to tensile or thermal loads can be detected using the AU method and could perhaps be used to determine when a specific metal matrix component is nearing its useful life and should be removed from service. Acousto-ultrasonics also appear to be sensitive to certain interface characteristics.

Sometimes, as in the case of the thermally cycled specimens, it is possible to identify a portion of the AU signal that is more sensitive to the mechanical property of interest than are other portions. When this is so one can take advantage of normalization. This can render the SWF less vulnerable to variability in factors such as transducer coupling.

The acousto-ultrasonic signal indicates that it may be possible to use the mean arrival time as a nondestructive monitor of tensile modulus in SiC/Ti-15-3 MMC specimens. More data are needed, which would include specimens having a wider range of modulus values, in order to assess the precision with which one can use SWF to predict modulus, although the initial results shown in this work are promising.

Future studies should be designed to enhance the high frequency part of the AU spectrum. This will allow the measurement of the second or higher harmonics in the signal and permit a more accurate calculation of the SWF. The higher harmonics should also be more sensitive to damage in the composite.

REFERENCES

1. Vary, A., E.R., Generazio, D.J., Roth, and G.Y., Baaklini, "Ultrasonic NDE of Structural Ceramics for Power and Propulsion Systems," Presented at the 4th European Conference on Non-Destructive Testing, London, England, September 13-18, 1987, Technical Memorandum, NASA TM-100147, 1987. Lewis Research Center, Cleveland, Ohio.

2. Vary, A., and K.F., Bowles, "Ultrasonic Evaluation of the Strength of Unidirectional Graphite Polyimide Composites," Proceedings of the Eleventh Symposium on Nondestructive Testing, 1977, pp. 242-258. ASNT, San Antonio, TX.

3. Kautz, H.E., "Ultrasonic Evaluation of Mechanical Properties of Thick, Multilayered, Filament-Wound Composites," Materials Evaluation, Vol. 45, Dec. 1987, pp. 1404-1412.

4. Kautz, H.E., "Acousto-Ultrasonic Verification of the Strength of Filament-Wound Composite Material," Presented at the Pressure Vessel Conference, ASME, Chicago, IL, July 21-24, 1986, Technical Memorandum, NASA TM-88827, 1986. Lewis Research Center, Cleveland, Ohio.

5. Hemann, J.H., P., Cavano, H., Kautz, and K., Bowles, "Trans-Ply Crack Density Detection by Acousto-Ultrasonics," Acousto-Ultrasonics, Theory and Application, 1988, pp. 319-326. Plenum Press, New York.

6. Lerch, B.A., T.P., Gabb, and R., MacKay, "A Heat Treatment Study of the SiC/Ti-15-3 Composite System," Technical Publication, NASA TP-2970, 1990. Lewis Research Center, Cleveland, Ohio.

7. Lerch, B.A., D.R., Hull, and T.A., Leonhardt, "Microstructure of a SiC/Ti-15-3 Composite," Composites, Vol. 21, May 1990, pp. 216-224.

8. Frederick, J.F., Ultrasonic Engineering, 1965, p. 363. John Wiley & Sons, Inc., New York.

9. Tang, B., E.G., Henneke II, and R.C., Stiffler, "Low Frequency Flexural Wave Propagation in Laminated Composite Plates," Acousto-Ultrasonics, Theory and Application, 1988, pp. 45-66. Plenum Press, New York.

10. Tang, B., and E.G., Henneke II, "Long Wavelength Approximation for Lamb Wave Characterization of Composite Laminates," Research in Nondestructive Evaluation, Vol. 1, 1989, pp. 51-64.

11. Vary, A., Materials Evaluation, "Correlations Among Ultrasonic Propagation Factors and Fracture Toughness Properties of Metallic Materials," Vol. 36, July 1979, pp. 55-64.

12. Vary, A., and D.R., Hull, "Interrelation of Material Microstructure Ultrasonic Factors, and Fracture-Toughness of a Two-Phase Titanium-Alloy," Materials Evaluation, Vol. 41, Mar. 1982, pp. 309-314.

13. Lerch, B.A., and J.F. Saltsman, "Tensile Deformation Damage in SiC Reinforced Ti-15V-3Cr-3Al-3Sn," NASA TM-103620, 1991.

14. Lerch, B.A., "Damage of a SiC/Ti-15V-3Al-3Sn-3Cr Composite Due to Thermal Excursion," HiTemp Review 1988: Advanced High Temperature Engine Materials Technology, Conference Publication, NASA CP-10025, 1988, pp. 139-144.

TABLE I. – THROUGH-THICKNESS LONGITUDINAL WAVE ULTRASONIC VELOCITY
CALCULATIONS FOR SiC/Ti-15-3, AND ALSO MONOLITHIC MATERIAL

Laminate code	Thickness, cm	First harmonic, MHz	Velocity[a], cm/μsec
$[0]_8$	0.21	3.11	0.66
$[\pm30]_{2s}$	.19	3.36	.65
$[\pm30]_{8s}$	.76	.86	.66
$[\pm45]_{2s}$	.19	3.30	.63
$[\pm60]_{2s}$	.19	3.33	.63
$[0/90]_{2s}$	.19	3.30	.63
$[90/0]_{2s}$	.20	3.27	.65
Ti-15-3 matrix	.11	5.10	.58
Ti metal	1.17	.49	.57
Estimate for 34 percent SiC and 66 percent Ti-15-3	----	----	.71

[a]Velocity calculated using equation (2).

TABLE II. – ROOM TEMPERATURE TENSILE PROPERTIES OF
SiC/Ti-15-3

Specimen number	E, GPa	Laminate code	Fiber, vol%	Heat treatment
2	181	$[0]_8$	33.9	None
3	192	$[0]_8$	34.8	700 °C/24 hr
4	178	$[0]_8$	33.6	700 °C/24 hr
5	258	$[0]_8$	34.1	700 °C/24 hr
6	193	$[0]_8$	33.6	None
7	183	$[0]_8$	34.0	700 °C/24 hr
8	179	$[0]_8$	33.4	None
9	197	$[0]_8$	35.4	700 °C/24 hr
10	150	$[\pm30]_{2s}$	34.4	700 °C/24 hr
11	150	$[\pm30]_{2s}$	33.7	700 °C/24 hr
12	152	$[\pm30]_{2s}$	34.4	700 °C/24 hr
13	149	$[\pm30]_{2s}$	34.5	700 °C/24 hr
14	129	$[\pm30]_{2s}$	34.3	None
15	142	$[\pm30]_{2s}$	34.5	None
16	141	$[\pm30]_{2s}$	34.3	None
18	148	$[\pm30]_{2s}$	34.2	700 °C/24 hr
A11	117	$[\pm45]_{2s}$	34.9	700 °C/24 hr
Fi	117	$[\pm60]_{2s}$	----	700 °C/24 hr
B2	148	$[0/90]_{2s}$	----	700 °C/24 hr
B4	159	$[0/90]_{2s}$	33.2	700 °C/24 hr
B11[a]	143	$[0/90]_{2s}$	----	700 °C/24 hr
C2[a]	138	$[90/0]_{2s}$	----	700 °C/24 hr

[a]Thermally cycled between 200 and 1000 °F for 2000 cycles.

TABLE III. – INTERRUPTED TENSILE TESTS OF SiC/Ti-15-3

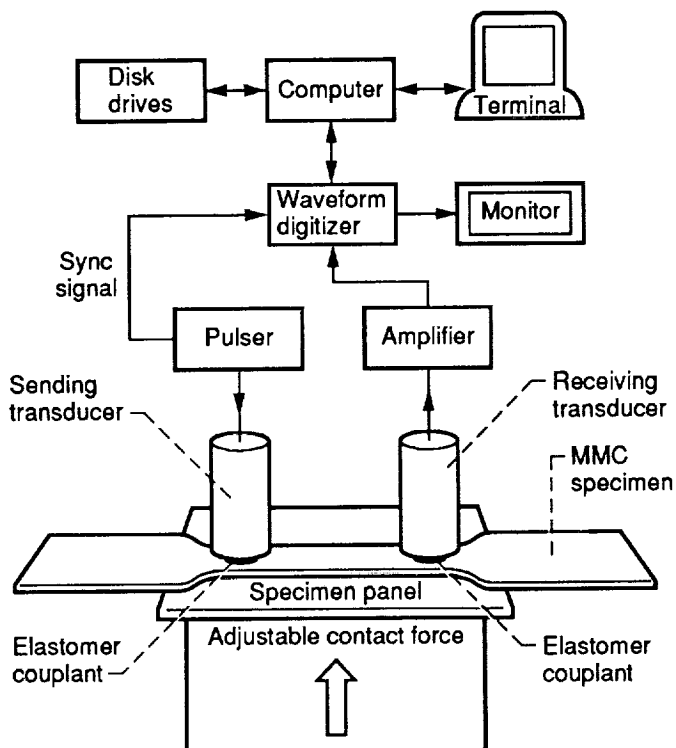| Specimen number	Laminate code	Strain at interruption, percent	Level of debonding
3	$[0]_8$	0.50	None detected
E6	$[0]_8$	.80	----------
E7	$[0]_8$	.85	Slight
39	$[90]_8$	.60	Slight
40	$[90]_8$	1.00	Extensive
10	$[\pm30]_{2s}$	.50	Slight
13	$[\pm30]_{2s}$	.61	Slight
D10	$[\pm30]_{2s}$	.80	Extensive

8

Figure 1.—Block diagram of the Acousto-ultrasonic and data processing system.
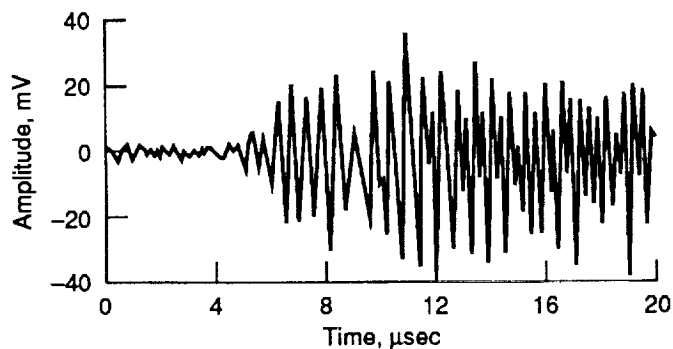

Figure 2.—Acousto-ultrasonic signal collected on SiC/Ti 15-3 tensile specimen with 5.0 MHz sending and 2.25 MHz receiving transducer.
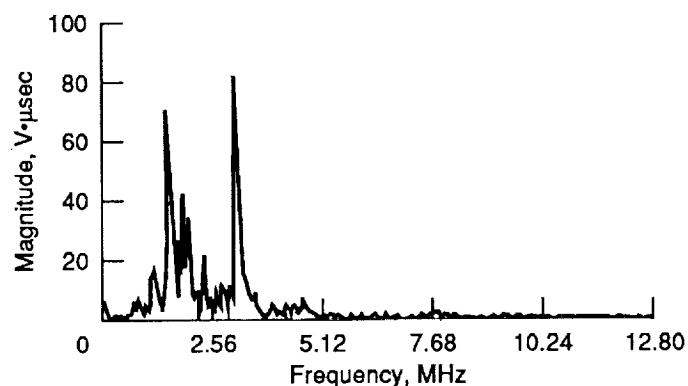

Figure 3.—Magnitude spectrum of the Acousto-ultrasonic signal in figure 2.
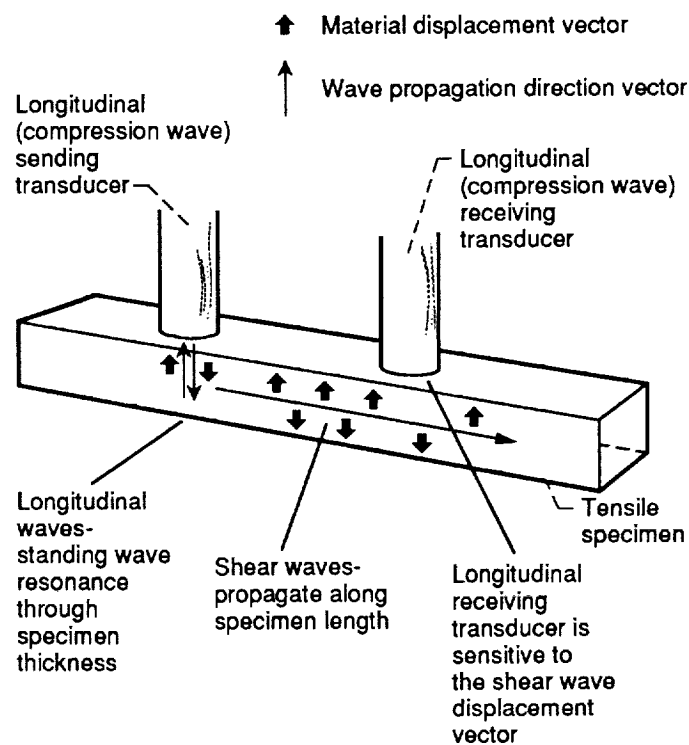

Figure 4.—Model for shear wave injection, propagation, and detection in the MMC tensile specimens.
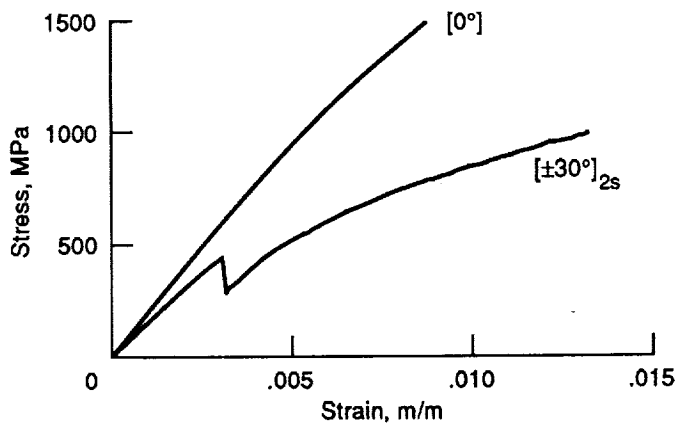
9

Figure 5.—Typical stress-strain curves for SiC/Ti 15-3 tensile specimens.
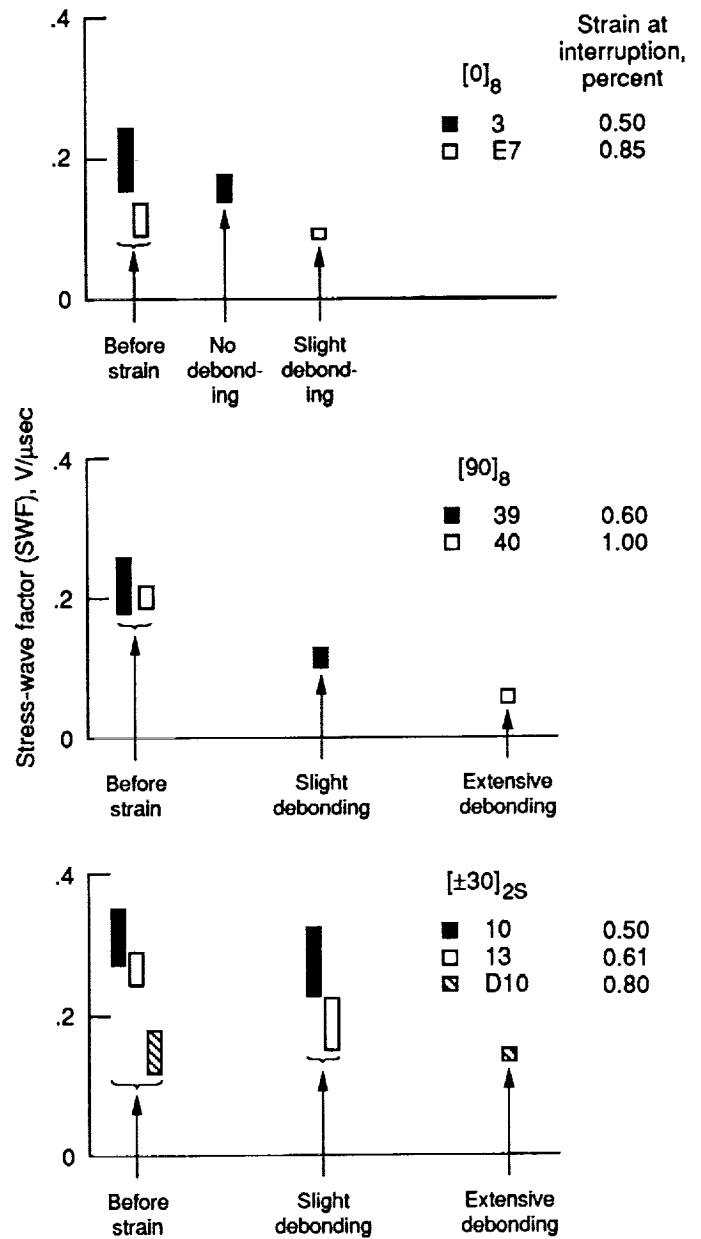

Figure 6.—Stress-wave factor versus degree of fiber/matrix debonding in the interrupted test specimens.
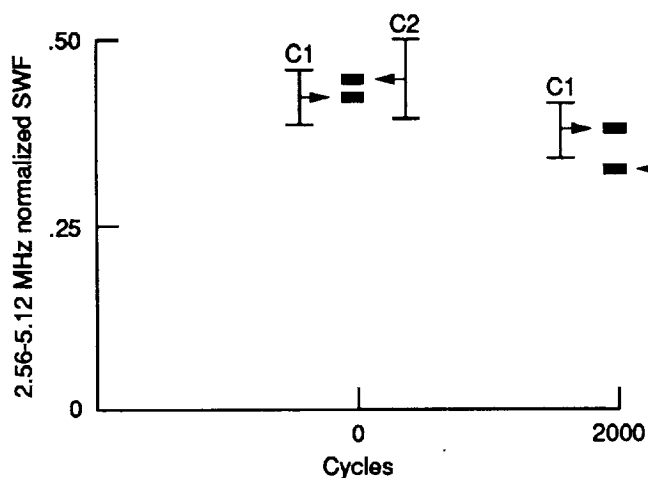
Figure 7.—Effect of thermal cycling on the stress-wave factor of the frequency range 2.56 to 5.12 MHz in [90/0] cross-ply specimens.
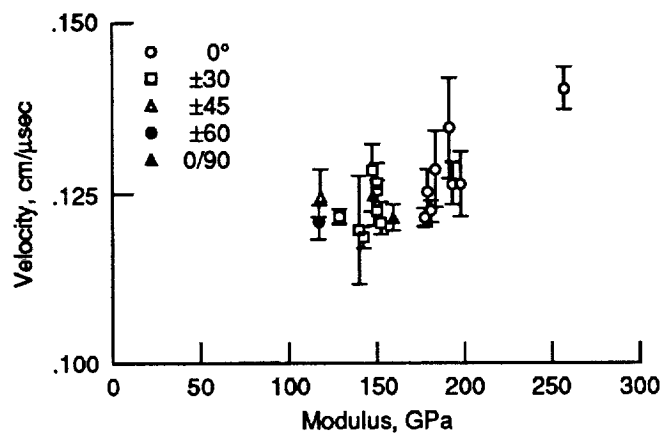
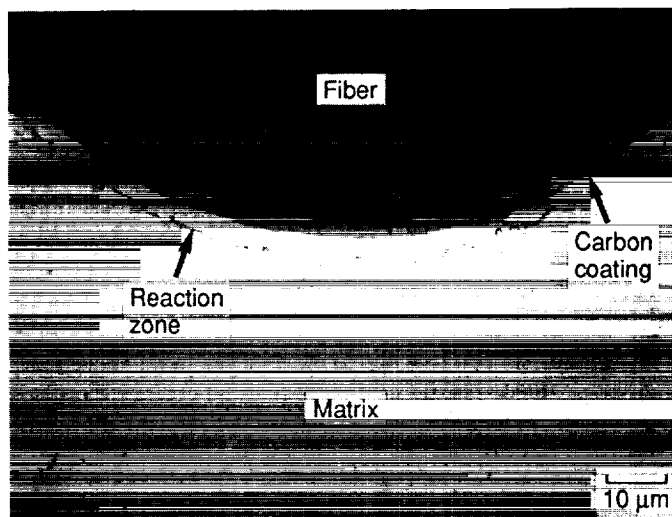Figure 8.—Effective Acousto-ultrasonic velocity (from equation (4)) versus tensile modulus.

Figure 9.—Micrograph of the atypical 3 μm thick reaction zone surrounding fibers in specimen #5.

11

NASA
National Aeronautics and
Space Administration

Report Documentation Page

1. Report No.	2. Government Accession No.	3. Recipient's Catalog No.
NASA TM -104339		

4. Title and Subtitle	5. Report Date
A Preliminary Investigation of Acousto-Ultrasonic NDE of Metal Matrix Composite Test Specimens	May 1991
	6. Performing Organization Code

7. Author(s)	8. Performing Organization Report No.
Harold E. Kautz and Brad A. Lerch	E -5651-1
	10. Work Unit No.
	510-01-01

9. Performing Organization Name and Address	11. Contract or Grant No.
National Aeronautics and Space Administration Lewis Research Center Cleveland, Ohio 44135 - 3191	
	13. Type of Report and Period Covered

12. Sponsoring Agency Name and Address	Technical Memorandum
National Aeronautics and Space Administration Washington, D.C. 20546 - 0001	14. Sponsoring Agency Code

15. Supplementary Notes

16. Abstract

Acousto-ultrasonic (AU) measurements were performed on a series of $[0]_8$, $[90]_8$, $[\pm 30]_{2s}$, $[\pm 45]_{2s}$, $[\pm 60]_{2s}$, $[0/90]_{2s}$, and $[90/0]_{2s}$ tensile specimens composed of eight laminated layers of continuous, SiC fiber reinforced Ti-15-3 matrix. The frequency spectrum was dominated by frequencies of longitudinal wave resonance through the thickness of the specimen at the sending transducer, while signal propagation from the sender to the receiver was by shear waves. The magnitude of the frequency spectrum of the AU signal was used for calculating a stress-wave factor (SWF) based upon integrating the spectral distribution function. The SWF was sensitive to fiber/matrix debonding due to mechanical strain and also to unconstrained thermal cycling. Damage in this MMC structure due to tensile loading or thermal cycling was detected by this change in the magnitude of the frequency spectrum. A measure of the speed of the acousto-ultrasonic pulse between the sending transducer and the receiver was obtained by calculating mean time, or first moment, in the time domain signal. This parameter shows some sensitivity to the stiffness of the tensile specimens. This sensitivity to stiffness needs further study.

17. Key Words (Suggested by Author(s))	18. Distribution Statement
Composite materials; Metal matrix composites; High temperature; Nondestructive tests; Ultrasonics; Mechanical properties; Tensile tests	Unclassified - Unlimited Subject Category 38

19. Security Classif. (of the report)	20. Security Classif. (of this page)	21. No. of pages	22. Price*
Unclassified	Unclassified	12	A03